Theoretical and Experimental Study of Tri- and Tetrahalodiorganostannate(IV) Salts. Solvent Dependence in the Reaction of Dimethyltin Dibromide with Tetraethylammonium Bromide

David Tudela,*[,†] Marcos Díaz,[†,‡] David A. Alvaro,[†] Joaquín Ignacio,[†] Luis Seijo,[§] and Vitaly K. Belsky[||]

Departamento de Química Inorgánica and Departamento de Química, Universidad Autónoma de Madrid, 28049-Madrid, Spain, and L. Ya. Karpov Physico-Chemical Institute, Obukha Str. 10, 103064 Moscow, Russia

Received September 19, 2000

The reaction of $SnMe_2Br_2$ with Et_4NBr, in a 1:2 molar ratio, yields $(Et_4N)_2[SnMe_2Br_4]$ (**1**) in $CHCl_3$/hexane mixtures but $(Et_4N)[SnMe_2Br_3]$ (**2**) in water. This remarkable solvent dependence is explained by means of a thermochemical cycle that includes the lattice enthalpies of both compounds, the solvation enthalpies of the Et_4N^+ and Br^- ions, and the gas-phase dissociation enthalpy of $[SnMe_2Br_4]^{2-}$ into $[SnMe_2Br_3]^-$ and Br^-. Both compounds have been characterized in the solid state by IR, Raman, and ^{119}Sn Mössbauer and MAS NMR spectroscopy and in solution by ^{1}H, ^{13}C, and ^{119}Sn NMR spectroscopy. The X-ray crystal structures of **1** and $(Me_4N)[SnMe_2Br_3]$ (**3**) are reported. The crystallographic study of **3** provides the first X-ray crystal structure containing an $[SnR_2Br_3]^-$ anion. The structures of $SnMe_2X_2$, $[SnMe_2X_3]^-$, *trans*-$[SnMe_2X_4]^{2-}$ (X = F, Cl, Br, I), *cis*-$[SnR_2Cl_4]^{2-}$ (R = Me, Et), $SnEt_2Cl_2$, $[SnEt_2Cl_3]^-$, and *trans*-$[SnEt_2Cl_4]^{2-}$ have been optimized, at the SCF level, by ab initio MO methods. The gas-phase formation of $[SnR_2X_3]^-$ anions from SnR_2X_2 and X^- is an exothermic process, but $[SnR_2X_4]^{2-}$ anions are unstable in the gas phase toward dissociation into $[SnR_2X_3]^-$ and X^-, while *cis*-$[SnR_2X_4]^{2-}$ species (R = Me, Et) are unstable with respect to their trans isomers by ca. 79 kJ/mol. The optimized gas-phase structures of $SnMe_2X_2$ show C−Sn−C angles increasing from 117.7 to 124.9° as the electronegativity of X increases. The pentacoordinated $[SnR_2X_3]^-$ anions show a trigonal-bipyramidal geometry with the R groups in equatorial positions (C−Sn−C angles in the range 128.7−133.5°) and longer Sn−X distances for the axial bonds than for the equatorial ones. When one takes into account that calculated distances are longer than the experimental ones, the present results strongly support the accuracy of the structural predictions from ab initio MO calculations.

Introduction

Tetrahalodiorganostannate(IV) anions, $[SnR_2X_4]^{2-}$, are among the simplest octahedral diorganotin species, and they can be considered as special cases of both tin(IV) halide complexes, SnX_4L_2 (L = R^-), and diorganotin dihalide complexes, $SnR_2X_2L_2$ (L = X^-). In the case of SnX_4L_2 complexes, salts of $[SnR_2X_4]^{2-}$ anions are the compounds with the longest Sn−X distances and the largest Mössbauer quadrupole splitting (QS) values, and they have been used in the correlations between both parameters.[1,2] Octahedral diorganotin dihalide complexes have been studied by several groups in recent years,[3,4] in part because some of these compounds display antitumor activity.[3d,5] Also, Tiekink and coworkers have compared the crystal structures of octahedral diorganotin dihalide complexes with those calculated by ab initio methods, in order to study the influence of crystal-packing effects on molecular structure.[4] Tetrahalodiorganostannate(IV) anions are very suitable for this kind of study, as they are very simple

* To whom correspondence should be addressed. Fax: +34-91-397-4833. E-mail: david.tudela@uam.es.
† Departamento de Química Inorgánica, Universidad Autónoma de Madrid.
‡ Current address: Instituto de Ciencia de Materiales de Madrid, CSIC, 28049-Madrid, Spain.
§ Departamento de Química, Universidad Autónoma de Madrid.
|| L. Ya. Karpov Physico-Chemical Institute.

(1) Tudela, D.; Khan, M. A.; Zuckerman, J. J. *J. Chem. Soc., Chem. Commun.* **1989**, 558.
(2) Tudela, D.; Tornero, J. D.; Monge, A.; Sánchez-Herencia, A. J. *Inorg. Chem.* **1993**, *32*, 3928.
(3) (a) Caruso, F.; Giomini, M.; Giuliani, A. M.; Rivarola, E. *J. Organomet. Chem.* **1996**, *506*, 67. (b) Alvarez Boo, P.; Casas, J. S.; Casellato, U.; Couce, M. D.; Freijanes, E.; Graziani, R.; Salgado, B.; Russo, U.; Sordo, J. *J. Organomet. Chem.* **1997**, *530*, 141. (c) Khoo, L. E.; Xu, Y.; Goh, N. K.; Chia, L. S.; Koh, L. L. *Polyhedron* **1997**, *16*, 573. (d) Teoh, S. G.; Ang, S. H.; Teo, S. B.; Fun, H. K.; Khew, K. L.; Ong, C. W. *J. Chem. Soc., Dalton Trans.* **1997**, 465. (e) Pettinari, C.; Pellei, M.; Miliani, M.; Cingolani, A.; Caseta, A.; Barba, L.; Pifferi, A.; Rivarola, E. *J. Organomet. Chem.* **1998**, *553*, 345. (f) Garoufis, A.; Koutsodimou, A.; Raptopoulou, C. P.; Simopoulos, A.; Katsaros, N. *Polyhedron* **1999**, *18*, 3005. (g) Tang, L. F.; Wang, Z. H.; Jia, W. L.; Xu, Y. M.; Wang, J. T. *Polyhedron* **2000**, *19*, 381. (h) Ghys, L.; Biesemans, M.; Gielen, M.; Garoufis, A.; Hadjiliadis, N.; Willem, R.; Martins, J. C. *Eur. J. Inorg. Chem.* **2000**, 513.
(4) (a) Buntine, M. A.; Hall, V. J.; Kosovel, F. J.; Tiekink, E. R. T. *J. Phys. Chem. A* **1998**, *102*, 2472. (b) Buntine, M. A.; Hall, V. J.; Kosovel, F. J.; Tiekink, E. R. T. *Z. Kristallogr.* **1998**, *213*, 669. (c) Tiekink, E. R. T.; Hall, V. J.; Hook, J.; Buntine, M. A. *Z. Kristallogr.* **2000**, *215*, 23.

10.1021/om000808s CCC: $20.00
Publication on Web 01/19/2001

species and they can provide information useful in understanding the structure and bonding of diorganotin dihalide complexes and hypervalency in organotin chemistry, a subject of current interest.[6]

The reaction of diorganotin dihalides with halide ions can yield not only $[SnR_2X_4]^{2-}$ but also $[SnR_2X_3]^-$ anions. For example, we have recently shown that the previously reported $[Bu^n_4N]_2$ $[SnMe_2I_4]$ is actually a 1:1 mixture of Bu^n_4NI and $[Bu^n_4N][SnMe_2I_3]$,[7] and it is interesting to learn about the factors that influence the crystallization of either type of salt. In the case of $[SnR_2X_4]^{2-}$ anions, many crystal structures with X = Cl (R = Me,[8] Et,[9] vinyl,[10] Ph[11]) are known, while for the other halides, only the crystal structures of $(NH_4)_2$-$[SnMe_2F_4]$,[12a] $(C_5H_5NH)_2[SnPh_2Br_4]$,[12b] and the zwitterionic species $[Me_2(ClCH_2)N(CH_2)_3]_2SnF_4$[12c] have been reported. In the case of $[SnR_2X_3]^-$ anions, only when X = Cl, there are crystal structures available in the literature.[8c,11d,13−16] While the crystal structures reported for $[SnPh_2Cl_3]^-$ anions,[11d,13] one structure containing $[SnEt_2Cl_3]^-$,[14a] and one structure containing $[SnMe_2Cl_3]^-$ [15] show isolated ions with the organic groups in the equatorial positions of a trigonal-bipyramidal structure, most $[SnMe_2Cl_3]^-$ anions are associated into dimers through more or less strong chlorine bridges.[8c,16] To improve our understanding of the energetic factors affecting the formation of $[SnR_2X_4]^{2-}$ and $[SnR_2X_3]^-$ anions, as well as the bonding and structural features of both kinds of anions, we have performed ab initio SCF MO calculations on the gas-phase structures of $SnMe_2X_2$, $[SnMe_2X_3]^-$, *trans*-$[SnMe_2X_4]^{2-}$ (X = F, Cl, Br, I), *cis*-$[SnR_2Cl_4]^{2-}$ (R = Me, Et), $SnEt_2Cl_2$, $[SnEt_2Cl_3]^-$, and *trans*-$[SnEt_2Cl_4]^{2-}$. The calculated gas-phase structures can show small bonding and structural trends that cannot be disclosed by the experimental X-ray crystal structures because of the strong influence of crystal-packing effects on the bond lengths and angles.[4,17,18] Given the scarcity of structural data for $[SnR_2Br_4]^{2-}$ and $[SnR_2Br_3]^-$ complexes, we have solved the crystal structure of one complex of each kind and compared the calculated gas-phase structures with the experimental solution and solid-state structures. The crystal structure of $(Me_4N)[SnMe_2Br_3]$ is the first one containing an $[SnR_2Br_3]^-$ anion. In addition, we have found and explained an interesting solvent dependence in the reaction of $SnMe_2Br_2$ with Et_4NBr, in a 1:2 molar ratio, that can give rise, according to the solvent, to $(Et_4N)_2$-$[SnMe_2Br_4]$ or $(Et_4N)[SnMe_2Br_3]$.

Experimental Section

General Procedures. Dimethyltin dibromide (mp 77−78 °C) was prepared by reaction of an aqueous HBr solution (48%) with a suspension of $SnMe_2O$ (K&K) in ethanol, in a 2:1 molar ratio, followed by vacuum elimination of the solvent and vacuum sublimation. It was characterized by IR and ^1H NMR spectroscopy.[19] The microanalyses (C, H, and N) were carried out with a Perkin-Elmer 2400 CHN elemental analyzer. ^1H, ^{13}C, and ^{119}Sn NMR spectra were recorded on a Bruker AMX-300 instrument, operating at 300.13, 75.47, and 111.89 MHz, respectively. Chemical shifts are referenced to $SiMe_4$ (^1H and ^{13}C) and $SnMe_4$ (^{119}Sn). Infrared spectra were recorded between 4000 and 200 cm^{-1} on a Perkin-Elmer 1650 FT-IR instrument, using Nujol mulls between CsI windows. Raman spectra were measured at room temperature on a Jarrell-Ash spectrophotometer, Model 25-300, using an Ar laser (5145 Å), with the polycrystalline samples sealed in capillary tubes. Mössbauer spectra at liquid-nitrogen temperature were obtained using the system and conditions described previously.[20] The sample thickness was 11 mg of natural tin per cm^2. The isomer shift is relative to $BaSnO_3$ at room temperature, and the reproducibility of the Mössbauer parameters was ±0.02 mm s^{-1}. ^{119}Sn MAS NMR spectra were obtained at room temperature in a Bruker MSL-400 spectrometer, using a standard single-pulse sequence. The external magnetic field was 9.4 T, and samples were spun at 12 kHz around an axis inclined 54°44′ with respect to this field. The spectrometer frequency was set to 149.11 MHz. For recorded spectra a $\pi/2$ pulse of 5 μs and a period between successive accumulations of 10 s were used. The number of scans was 800. Chemical shift values were referenced to $SnMe_4$. The analysis of ^{119}Sn MAS NMR spectra

(5) (a) Crowe, A. J.; Smith, P. J.; Atassi, G. *Chem.-Biol. Interact.* **1980**, *32*, 171. (b) Crowe, A. J.; Smith, P. J.; Atassi, G. *Inorg. Chim. Acta* **1984**, *93*, 179. (c) Crowe, A. J.; Smith, P. J.; Cardin, C. J.; Parge, H. E.; Smith, F. E. *Cancer Lett.* **1984**, *24*, 45. (d) Kavanos, T. A.; Keramidas, A. D.; Mentzafos, D.; Russo, U.; Terzis, A.; Tsangaris, J. M. *J. Chem. Soc., Dalton Trans.* **1992**, 2729. (e) Gielen, M.; Lelieveld, P.; de Vos, D.; Willem, R. In *Metal Complexes in Cancer Chemotherapy*; Keppler, B. K., Ed.; VCH: Weinheim, Germany, 1993; pp 381−390. (f) Gielen, M. *Coord. Chem. Rev.* **1996**, *151*, 41. (g) de Vos, D.; Willem, R.; Gielen, M.; van Wingerden, K. E.; Nooter, K. *Metal Based Drugs* **1998**, *5*, 179. (h) Clarke, M. J.; Zhu, F.; Frasca, D. R. *Chem. Rev.* **1999**, *99*, 2511.

(6) (a) Kolb, U.; Dräger, M.; Dargatz, M.; Jurkschat, K. *Organometallics* **1995**, *14*, 2827. (b) Pieper, N.; Klaus-Mrestani, C.; Schürmann, M.; Jurkschat, K.; Biesemans, M.; Verbruggen, I.; Martins, J. C.; Willem, R. *Organometallics* **1997**, *16*, 1043. (c) Mehring, M.; Schürmann, M.; Jurkschat, K. *Organometallics* **1998**, *17*, 1227. (d) Mehring, M.; Löw, C.; Schürmann, M.; Jurkschat, K. *Eur. J. Inorg. Chem.* **1999**, 887.

(7) Tudela, D.; Sánchez-Herencia, A. J.; Díaz, M.; Fernández-Ruiz, R.; Menéndez, N.; Tornero, J. D. *J. Chem. Soc., Dalton Trans.* **1999**, 4019.

(8) (a) Smart, L. E.; Webster, M. *J. Chem. Soc., Dalton Trans.* **1976**, 1924. (b) Nasser, F. A. K.; Hossain, M. B.; Van der Helm, D.; Zuckerman, J. J. *Inorg. Chem.* **1984**, *23*, 606. (c) Matsubayashi, G. E.; Ueyama, K.; Tanaka, T. *J. Chem. Soc., Dalton Trans.* **1985**, 465. (d) Valle, G.; Sánchez-González, A.; Ettore, R.; Plazzogna, G. *J. Organomet. Chem.* **1988**, *348*, 49. (e) Casellato, U.; Graziani, R.; Martelli, M.; Plazzogna, G. *Acta Crystallogr., Sect. C* **1995**, *51*, 2293. (f) Casas, J. S.; Castiñeiras, A.; Martinez, G.; Sordo, J.; Varela, J. M.; Couce, M. D. *Acta Crystallogr., Sect. C* **1995**, *51*, 2561. (g) Francisco, R. H. P.; Moreno, P. C.; Gambardella, M. T. do P.; de Sousa, G. F.; Mangas, M. B. P.; Abras, A. *Acta Crystallogr., Sect. C* **1998**, *54*, 1444.

(9) Ueyama, K.; Matsubayashi, G. E.; Shimizu, R.; Tanaka, T. *Polyhedron* **1985**, *4*, 1783.

(10) Hall, V. J.; Tiekink, E. R. T. *Acta Crystallogr., Sect. C* **1996**, *52*, 2143.

(11) (a) Teoh, S. G.; Teo, S. B.; Yeap, G. Y.; Declercq, J. P. *Polyhedron* **1992**, *11*, 2351. (b) Casas, J. S.; Castiñeiras, A.; Couce, M. D.; Martinez, G.; Sordo, J.; Varela, J. M. *J. Organomet. Chem.* **1996**, *517*, 165. (c) Hazell, A.; Khoo, L. E.; Ouyang, J.; Rausch, B. J.; Tavares, Z. M. *Acta Crystallogr., Sect. C* **1998**, *54*, 728. (d) Ouyang, J.; Xu, Y.; Khoo, L. E. *J. Organomet. Chem.* **1998**, *561*, 143.

(12) (a) Tudela, D. *J. Organomet. Chem.* **1994**, *471*, 63. (b) Tudela, D.; Khan, M. A. *J. Chem. Soc., Dalton Trans.* **1991**, 1003. (c) Pieper, N.; Ludwig, R.; Schürmann, M.; Jurkschat, K.; Biesemans, M.; Verbruggen, I.; Willem, R. *Phosphorus, Sulfur Silicon Relat. Elem.* **1999**, *150−151*, 305.

(13) García Martínez, E.; Sánchez González, A.; Castiñeiras, A.; Casas, J. S.; Sordo, J. *J. Organomet. Chem.* **1994**, *469*, 41.

(14) (a) Mazza, P.; Orcesi, M.; Pellizi, G.; Predieri, G.; Zani, F. *J. Inorg. Biochem.* **1992**, *48*, 251. (b) Matsubayashi, G.; Shimizu, R.; Tanaka, T. *J. Chem. Soc. Dalton Trans.* **1987**, 1793.

(15) Einstein, F. W. B.; Penfold, B. R. *J. Chem. Soc. (A)* **1968**, 3019.

(16) (a) Lanfranchi, M.; Pellinghelli, M. A.; Vasapollo, G.; Nobile, C. F. *J. Crystallogr. Spectrosc. Res.* **1986**, *16*, 863. (b) Jones, R.; Warrens, C. P.; Williams, D. J.; Woollins, J. D. *J. Chem. Soc., Dalton Trans.* **1987**, 907. (c) Teoh, S. G.; Teo, S. B.; Yeap, G. Y.; Fun, H. K. *J. Organomet. Chem.* **1992**, *439*, 139. (d) Buttenshaw, A. J.; Duchene, M.; Webster, M. *J. Chem. Soc., Dalton Trans.* **1975**, 2230. (e) Hitchcock, P. B.; Klein, S. I.; Nixon, J. F. *J. Organomet. Chem.* **1983**, *241*, C9.

(17) Tiekink, E. R. T.; Hall, V. J.; Buntine, M. A. *Z. Kristallogr.* **1999**, *214*, 124.

(18) Martín, A.; Orpen, A. G. *J. Am. Chem. Soc.* **1996**, *118*, 1464.

(19) Petrosian, V. S. *Prog. NMR Spectrosc.* **1977**, *11*, 115.

(20) (a) Tudela, D.; Fernández, V.; Tornero, J. D. *Z. Anorg. Allg. Chem.* **1984**, *509*, 174. (b) Tudela, D.; Fernández, V.; Tornero, J. D. *Inorg. Chem.* **1985**, *24*, 3892.

was done with the WINFIT program.[21] In this program the principal values of the chemical shift anisotropy tensor were determined from the intensity of sidebands by Herzfeld and Berger's method.[22] The parameters are reported as the isotropic chemical shift ($\delta_{iso} = -\sigma_{iso} = -^1/_3(\sigma_{xx} + \sigma_{yy} + \sigma_{zz})$) (ppm), the anisotropy ($\Delta\sigma = \sigma_{zz} - {}^1/_2(\sigma_{xx} + \sigma_{yy})$) (ppm), and the asymmetry ($\eta = {}^3/_2(\sigma_{yy} - \sigma_{xx})(\Delta\sigma)^{-1}$). The three components of the shielding tensor (σ_{xx}, σ_{yy}, and σ_{zz}), within the principal axis system, are defined such that $|\sigma_{zz} - \sigma_{iso}| \geq |\sigma_{xx} - \sigma_{iso}| \geq |\sigma_{yy} - \sigma_{iso}|$.

Synthesis of Tetraethylammonium Tetrabromodimethylstannate(IV) (1). Hexane (60 mL) was layered onto a solution containing 0.40 g of $SnMe_2Br_2$ (1.30 mmol) and 0.55 g of Et_4NBr (2.62 mmol) in $CHCl_3$ (15 mL), and a white precipitate was formed immediately. After the mixture stood for 15 h, the solid was filtered off, washed twice with hexane (10 mL), and dried in air, yielding 0.76 g (80%) of crude **1**. Colorless crystals (85% yield) were obtained by vapor diffusion of pentane into a chloroform solution of **1**. Mp: 191−192 °C. ^{1}H NMR ($CDCl_3$; δ, ppm): 3.44 [q, 16H, CH_3CH_2N, $^3J(^1H-^1H) = 7.3$ Hz], 1.71 [s, 6H, Me_2Sn, $^2J(^{119}Sn-^1H) = 85.1$ Hz, $^2J(^{117}Sn-^1H) = 81.4$ Hz], 1.39 [tt, 24H, CH_3CH_2N, $^3J(^1H-^1H) = 7.3$ Hz, $^3J(^{14}N-^1H) = 1.8$ Hz]. ^{1}H NMR (D_2O, δ ppm): 3.22 [q, 16H, CH_3CH_2N, $^3J(^1H-^1H) = 7.3$ Hz], 1.22 [tt, 24H, CH_3CH_2N, $^3J(^1H-^1H) = 7.3$ Hz, $^3J(^{14}N-^1H) = 1.9$ Hz], 0.96 [s, 6H, Me_2Sn, $^2J(^{119}Sn-^1H) = 107.7$ Hz, $^2J(^{117}Sn-^1H) = 102.9$ Hz]. ^{13}C NMR ($CDCl_3$; δ, ppm): 52.9 (CH_3CH_2N), 22.5 [Me_2Sn, $^1J(^{119}Sn-^{13}C) = 658$ Hz, $^1J(^{117}Sn-^{13}C) = 628$ Hz], 8.0 (CH_3CH_2N). ^{119}Sn NMR ($CDCl_3$; δ, ppm): − 144.1. ^{119}Sn NMR (D_2O; δ, ppm): −324.9. IR data (Nujol; cm^{-1}): 568 m, ν_{as}(Sn−C). Raman data (cm^{-1}): 500 vs, ν_s(Sn−C). ^{119}Sn Mössbauer (mm s^{-1}): IS = 1.58, QS = 3.89, $\Gamma_1 = 0.82$, $\Gamma_2 = 0.83$. Anal. Calcd for $C_{18}H_{46}Br_4N_2Sn$: C, 29.66; H, 6.36; N, 3.84. Found: C, 29.50; H, 6.25; N, 3.78.

Synthesis of Tetraethylammonium Tribromodimethylstannate(IV) (2). A solution containing tetraethylammonium bromide (0.60 g, 1.94 mmol) and dimethyltin dibromide (0.41 g, 1.94 mmol), in ca. 10 mL of water, was allowed to evaporate until the compound crystallized as colorless plates (0.66 g, 65%). Mp: 166−167 °C. ^{1}H NMR ($CDCl_3$; δ, ppm): 3.38 [q, 8H, CH_3CH_2N, $^3J(^1H-^1H) = 7.3$ Hz], 1.68 [s, 6H, Me_2Sn, $^2J(^{119}Sn-^1H) = 83.1$ Hz, $^2J(^{117}Sn-^1H) = 79.5$ Hz], 1.39 [tt, 12H, CH_3CH_2N, $^3J(^1H-^1H) = 7.3$ Hz, $^3J(^{14}N-^1H) = 1.9$ Hz]. ^{1}H NMR (D_2O; δ, ppm): 3.22 [q, 8H, CH_3CH_2N, $^3J(^1H-^1H) = 7.3$ Hz], 1.22 [tt, 12H, CH_3CH_2N, $^3J(^1H-^1H) = 7.3$ Hz, $^3J(^{14}N-^1H) = 1.9$ Hz], 0.96 [s, 6H, Me_2Sn, $^2J(^{119}Sn-^1H) = 107.8$ Hz, $^2J(^{117}Sn-^1H) = 103.1$ Hz]. ^{13}C NMR ($CDCl_3$; δ, ppm): 53.0 (CH_3CH_2N), 21.2 [Me_2Sn, $^1J(^{119}Sn-^{13}C) = 638$ Hz, $^1J(^{117}Sn-^{13}C) = 609$ Hz], 8.0 (CH_3CH_2N). ^{119}Sn NMR ($CDCl_3$; δ, ppm): −118.8. ^{119}Sn NMR (D_2O; δ, ppm): −322.3. IR data (Nujol; cm^{-1}): 566 m, ν_{as}(Sn−C); 514 w, ν_s(Sn−C); 219 m, ν(Sn−Br). Raman data (cm^{-1}): 569 w, ν_{as}(Sn−C); 516 vs, ν_s(Sn−C); 221 s, ν(Sn−Br). ^{119}Sn Mössbauer (mm s^{-1}): IS = 1.53, QS = 3.46, $\Gamma_1 = 0.76$, $\Gamma_2 = 0.84$. Anal. Calcd for $C_{10}H_{26}Br_3NSn$: C, 23.15; H, 5.05; N, 2.70. Found: C, 22.92; H, 4.69; N, 2.50. The same compound was formed when the reaction between $SnMe_2Br_2$ and Et_4NBr was performed in a 1:2 molar ratio.

Synthesis of Tetramethylammonium Tribromodimethylstannate(IV) (3). A solution containing tetramethylammonium bromide (0.17 g, 1.10 mmol) and dimethyltin dibromide (0.33 g, 1.07 mmol) in ca. 15 mL of water was allowed to evaporate until the compound crystallized as colorless plates (0.44 g, 89%). Mp: 211−213 °C. ^{1}H NMR (D_2O; δ, ppm): 3.16 [s, 12H, CH_3N], 0.96 [s, 6H, Me_2Sn, $^2J(^{119}Sn-^1H) = 107.5$ Hz]. IR data (Nujol; cm^{-1}): 564 s, ν_{as}(Sn−C); 521 m, ν_s(Sn−C); 218 vs, ν(Sn−Br). Raman data (cm^{-1}): 562 w, ν_{as}(Sn−C); 520 vs, ν_s(Sn−C); 221 m, ν(Sn−Br). Anal. Calcd for $C_6H_{18}Br_3NSn$: C, 15.58; H, 3.92; N, 3.03. Found: C, 15.97; H, 3.81; N, 3.22. The same compound was obtained when the reaction was performed in a 2:1 molar ratio.

Table 1. Crystallographic Data for Compounds 1−3

	1	**2**	**3**
formula	$C_{18}H_{46}Br_4N_2Sn$	$C_{10}H_{26}Br_3NSn$	$C_6H_{18}Br_3NSn$
fw	728.90	518.74	462.63
cryst size, mm	0.47 × 0.44 × 0.30	0.56 × 0.28 × 0.06	0.46 × 0.41 × 0.14
cryst syst	monoclinic	orthorhombic	orthorhombic
space group (No.)	$P2_1/n$ (14)	*Pccn* (56)	*Pbcm* (57)
a, Å	10.627(2)	10.778(2)	6.504(1)
b, Å	10.466(2)	12.373(2)	11.678(2)
c, Å	12.931(3)	13.397(3)	18.740(4)
β, deg	94.21(3)	90	90
V, Å^3	1434.3(5)	1786.6(6)	1423.4(4)
Z	2	4	4
D_{calcd}, g cm^{-3}	1.688	1.929	2.159
μ, mm^{-1}	6.468	8.119	10.176
F(000)	716	992	864
θ range, deg	2.40−24.97	2.51−24.92	3.49−26.96
no. of data/ restraints/params	1173/0/116		530/0/58
R1[a]	0.0448		0.0473
wR2[b]	0.1066		0.1237
goodness of fit	1.080		0.965
largest diff peak, e/Å^3	1.22		1.20

[a] $R1 = \sum||F_o| - |F_c||/\sum|F_o|$. [b] $wR2 = [\sum w(F_o^2 - F_c^2)^2/\sum wF_o^4]^{1/2}$.

X-ray Crystallography. The details of crystal data collection and parameter refinement for **1**−**3** are collected in Table 1. Crystals of **1** were obtained by vapor diffusion of pentane into a chloroform solution, while crystals of **2** and **3** were obtained directly from the reaction mixture. Crystals of **2** were affected by severe disorder or twinning problems, and a satisfactory solution of the structure could not be obtained. Diffraction data were collected at 293 K on an Enraf-Nonius CAD-4 diffractometer, using Nb-filtered Mo Kα radiation (λ = 0.710 73 Å) with $\theta/2\theta$ scans. Diffractometer data were processed by the program PROFIT[23] with profile analysis of reflections. After corrections for Lorentz and polarization factors, the structure was solved by the heavy-atom method using the SHELXTL package.[24a] After that, all reflections with $I < 3\sigma(I)$ ($<2\sigma(I)$ for **3**) were excluded from calculations. Refinement was done by full-matrix least squares based on F^2 using the SHELX-97 package.[24b] All non-hydrogen atoms were refined anisotropically. Hydrogen atoms were located in a difference map for **1** (placed in calculated positions for **3**) and included in the refinement with fixed coordinates and thermal parameters. Extinction and numeric absorption corrections were made.[25] T_{min}/T_{max} values were 0.089/0.185 and 0.038/0.263 for **1** and **3**, respectively. Scattering factors were obtained from ref 26.

Computational Details. Geometry optimizations were performed at the SCF level with the software package MOLCAS-4.1,[27] on an Alpha Server 8400 5/300 and an Alpha Station 500 at the CCCFC of the Universidad Autónoma de

(21) Massiot, D.; Thiele, H.; Germanus, A. *Bruker Rep.* **1994**, *140*, 43.
(22) Herzfeld, J.; Berger, A. E. *J. Chem. Phys.* **1980**, *73*, 6021.
(23) Strel'tsov, V. A.; Zavodnik, V. E. *Kristallografiya* **1989**, *34*, 1369.
(24) (a) Sheldrick, G. M. *SHELXTL User Manual*, Revision 3; Nicolet XRD: Cupertino, CA, 1981. (b) Sheldrick, G. M. SHELX-97; University of Göttingen, Göttingen, Germany, 1997.
(25) Axelrud, L. G.; Grin, Yu. N.; Zavalii, P. Yu.; Pecharsky, V. K.; Fundamensky, V. S. CSD: Universal Program Package for Single Crystal and/or Powder Structure Data Treatment. *Collected Abstracts*, 12th European Crystallographic Meeting; Moscow, Aug 1989; USSR Academy of Sciences: Moscow, 1989; p 155.
(26) *International Tables for X-ray Crystallography*; Kynoch Press: Birmingham, U.K., 1974; Vol. IV.
(27) Andersson, K.; Blomberg, M. R. A.; Fülscher, M. P.; Karlström, G.; Lindh, R.; Malmqvist, P. Å.; Neogrády, P.; Olsen, J.; Roos, B. O.; Sadlej, A. J.; Schütz, M.; Seijo, L.; Serrano-Andrés, L.; Siegbahn, P. E. M.; Widmark, P. O. MOLCAS, Version 4.1; Lund University, Lund, Sweden, 1997.

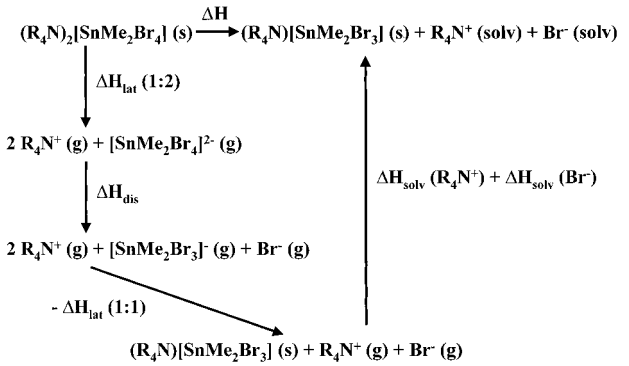

Figure 1. Thermochemical cycle for the crystallization of **1** or **2**.

Madrid. Cowan-Griffin[28] based relativistic core ab initio model potentials (effective core potentials) were used for Sn ([Kr]-core),[29] F ([He]-core),[30] Cl ([Ne]-core),[30] Br ([Ar, 3d]-core),[30] I ([Kr]-core),[29] and C ([He]-core),[30] together with Gaussian basis sets of size (11s10p7d)/[3s3p3d] for Sn,[29] (5s6p1d)/[3s4p1d] for F,[30] (7s7p1d)/[3s5p1d] for Cl,[30] (9s8p4d)/[3s4p2d] for Br,[30] (11s10p7d)/[3s4p3d] for I,[29] (5s5p1d)/[2s3p1d] for C, and (6s2p)/[4s2p] for H.[31] The calculations were carried out using C_{2h} symmetry for *trans*-$[SnMe_2X_4]^{2-}$ (X = F, Cl, Br, I) ions and C_{2v} for all the other molecules and ions.

Results and Discussion

Solvent Dependence in the Reaction of Dimethyltin Dibromide with Tetraethylammoniom Bromide and Spectroscopic Characterization of the Products. The reaction of $SnMe_2Br_2$ with Et_4NBr, in a 1:2 molar ratio, yields $(Et_4N)_2[SnMe_2Br_4]$ (**1**) in $CHCl_3$/hexane mixtures but $(Et_4N)[SnMe_2Br_3]$ (**2**) in water. Complex **2** had been prepared previously by Clark and Wilkins from dry ethanol, by mixing the components in a 1:1 proportion.[32] This remarkable solvent dependence can be understood with the help of the thermochemical cycle shown in Figure 1, where $\Delta H_{lat}(1:2)$ and $\Delta H_{lat}(1:1)$ are the lattice enthalpies of **1** and **2**, respectively. Figure 1 shows that high solvation enthalpies for Et_4N^+ and Br^- will favor the crystallization of **2** and, therefore, low solvation enthalpies would favor the crystallization of **1**. For that reason, when the reaction is performed in a highly solvating solvent such as water, complex **2** crystallizes, but in solvents with a low solvating power such as $CHCl_3$/hexane mixtures **1** is formed. A more quantitative analysis of the cycle shown in Figure 1 will be given at the end of this paper, after evaluation of ΔH_{dis} from the ab initio MO calculations.

The compounds **1** and **2** can be easily distinguished in the solid state by a variety of techniques. The simplest one is vibrational spectroscopy, because the octahedral centrosymmetrical $[SnMe_2Br_4]^{2-}$ anions (idealized D_{4h} symmetry) show only one tin−carbon stretching vibration in the IR and Raman spectra, with mutual exclusion, while the trigonal-bipyramidal $[SnMe_2Br_3]^-$ anion (idealized C_{2v} symmetry) shows two ν(Sn−C) bands in the IR and Raman spectra, with concordance of activities (see Experimental Section). The above conclusion would not be altered if $[SnMe_2Br_3]^-$ anions were associated into dimers as most $[SnMe_2Cl_3]^-$ anions are,[8c,16] because the bent C−Sn−C arrangement would also lead to the appearance of two ν(Sn−C) bands in the IR and Raman spectra.

Table 2. MAS ^{119}Sn NMR Parameters (in ppm[a]) for 1 and 2

compd	δ_{iso}	$\Delta\sigma$	η	σ_{xx}	σ_{yy}	σ_{zz}
1	−305	−398	0	438	438	40
2	−135	451	0.8	−136	105	435

[a] Except for η, which is dimensionless.

The Mössbauer parameters for **1** (IS = 1.58, QS = 3.89 mm s^{-1}) and **2** (IS = 1.53, QS = 3.46 mm s^{-1}) show a similar isomer shift value and a higher quadrupole splitting for the octahedral anion. According to the published correlation between C−Sn−C angles and QS values,[34] the calculated C−Sn−C angles for **1** and **2** are 158 and 141°, respectively. In the case of **1**, the calculated angle differs by 22° from the 180° expected from the mutual exclusion of ν_{as}(Sn−C) and ν_s(Sn−C) in the IR and Raman spectra and confirmed crystallographically (see below). Such a difference illustrates the limitations of the structural predictions based on the C−Sn−C angle vs QS correlation, for which we had previously found differences of 15°.[12b] The QS of **1** leads to a calculated average Sn−Br distance of 2.78 ± 0.02 Å according to the correlation between partial quadrupole splitting data and Sn−Br distances for $SnBr_4L_2$ complexes.[2] The Mössbauer parameters of **2** agree with those reported previously by Parish and Platt.[35]

The MAS ^{119}Sn NMR parameters for **1** and **2** are collected in Table 2. The values of the isotropic chemical shift show an increased shielding for **1**, in agreement with its higher coordination number.[36] It has been reported that the ^{119}Sn chemical shifts in related di-*n*-butyltin(IV) compounds range from −90 to −190 ppm, for coordination number 5, and from −210 to −400 ppm, for coordination number 6.[37] The isotropic chemical shifts, −305 ppm for **1** and −135 ppm for **2**, are in the middle of the ranges corresponding to coordination numbers 6 and 5, respectively. It is interesting to note that the isotropic chemical shift for **2** is not close to the limit corresponding to hexacoordinated complexes, so that it could have a structure containing isolated anions, in contrast to the structures observed for $[SnMe_2Cl_3]^-$ anions that are generally associated as dimers.[8c,16]

The MAS ^{119}Sn NMR spectra of **1** and **2** show a strong anisotropy, $\Delta\sigma$ (see Table 2), in agreement with the expected structures: octahedral for $[SnMe_2Br_4]^{2-}$ and trigonal bipyramidal for $[SnMe_2Br_3]^-$. The $[SnMe_2Br_4]^{2-}$ anions have axial symmetry ($\sigma_{xx} = \sigma_{yy}$) and they do not present asymmetry ($\eta = 0$), while the $[SnMe_2Br_3]^-$ anions (idealized symmetry C_{2v}) do not have axial symmetry and present a strong asymmetry ($\eta = 0.8$). Furthermore, the anisotropy has a different sign in both compounds. The negative sign of $\Delta\sigma$ for **1** means that the tin nucleus is less shielded in the *z* direction (Sn−C

(28) Cowan, R. D.; Griffin, D. C. *J. Opt. Soc. Am.* **1976**, *66*, 1010.
(29) Barandiaran, Z.; Seijo, L. *J. Chem. Phys.* **1994**, *101*, 4049.
(30) Barandiaran, Z.; Seijo, L. *Can. J. Chem.* **1992**, *70*, 409.
(31) Huzinaga, S. *J. Chem. Phys.* **1965**, *42*, 1293.
(32) Clark, J. P.; Wilkins, C. J. *J. Chem. Soc. A* **1966**, 871.
(33) (a) Parish, R. V. *Prog. Inorg. Chem.* **1972**, *15*, 101. (b) Bancroft, G. M.; Platt, R. H. *Adv. Inorg. Chem. Radiochem.* **1972**, *15*, 59.
(34) (a) Sham, T. K.; Bancroft, G. M. *Inorg. Chem.* **1975**, *14*, 2281. (b) Parish, R. V. In *Mössbauer Spectroscopy Applied to Inorganic Chemistry*; Long, G. J., Ed.; Plenum: New York, 1984; Chapter 16.
(35) Parish, R. V.; Platt, R. H. *Inorg. Chim. Acta* **1970**, *4*, 65.
(36) Wrackmeyer, B. *Annu. Rep. NMR Spectrosc.* **1985**, *16*, 73.
(37) Holeček, J.; Nádvorník, M.; Handlíř, K.; Lyčka, A. *J. Organomet. Chem.* **1986**, *315*, 299.

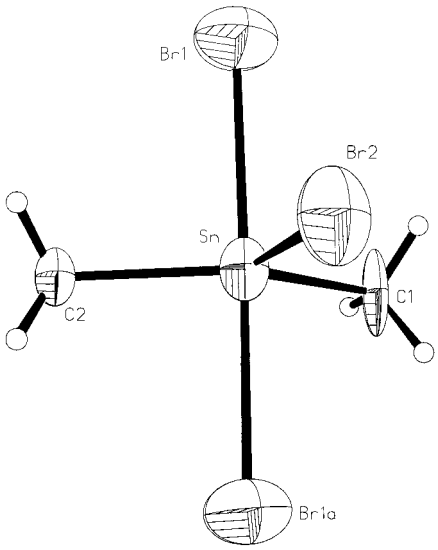

Figure 2. ORTEP plot of the $[SnMe_2Br_3]^-$ anion in $(Me_4N)[SnMe_2Br_3]$ (**3**). Thermal ellipsoids are drawn at the 50% probability level.

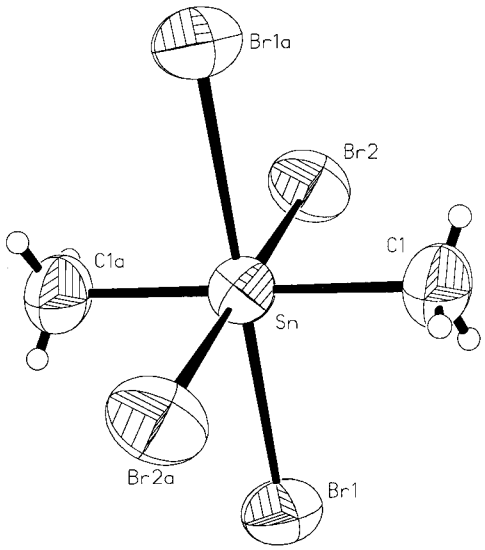

Figure 3. ORTEP plot of the $[SnMe_2Br_4]^{2-}$ anion in $(Et_4N)_2[SnMe_2Br_4]$ (**1**). Thermal ellipsoids are drawn at the 50% probability level.

Table 3. Selected Bond Lengths (Å) and Angles (deg) for 3[a]

Sn−Br(1)	2.734(2)	Sn−Br(2)	2.498(3)
Sn−C(1)	2.14(2)	Sn−C(2)	2.15(3)
C(1)−Sn−C(2)	133.2(8)	C(1)−Sn−Br(2)	111.4(4)
C(2)−Sn−Br(2)	115.4(6)	C(1)−Sn−Br(1)	90.86(4)
C(2)−Sn−Br(1)	89.40(6)	Br(1)−Sn−Br(2)	89.70(6)
Br(1)−Sn−Br(1)'	178.28(8)		

[a] Symmetry code (′): $x, y, 1/2 - z$.

Table 4. Selected Bond Lengths (Å) and Angles (deg) for 1[a]

Sn−Br(1)	2.7666(10)	Sn−Br(2)	2.7696(11)
Sn−C(1)	2.137(8)		
C(1)−Sn−Br(1)	90.2(3)	C(1)−Sn−Br(2)	90.5(3)
C(1)−Sn−C(1)′	180	Br(1)−Sn−Br(2)	90.24(4)

[a] Symmetry code (′): $1 - x, 1 - y, 1 - z$.

bonds) than in the *x* and *y* directions (Sn−Br bonds). In conclusion, MAS ^{119}Sn NMR is an excellent technique to distinguish between $[SnR_2X_4]^{2-}$ and $[SnR_2X_3]^-$ anions, not only because the isotropic chemical shift values indicate the coordination number of tin but also because of the different pattern of the shielding tensors, with axial symmetry for $[SnR_2X_4]^{2-}$ and significant asymmetry for $[SnR_2X_3]^-$. Although the MAS ^{119}Sn NMR parameters of $(Et_4N)[SnMe_2Br_3]$ (**2**) suggest that this compound could have isolated trigonal-bipyramidal anions, severe twinning or disorder problems prevented a crystallographic confirmation of this structure. However, we could solve the crystal structure of the closely related compound $(Me_4N)[SnMe_2Br_3]$ (**3**), previously prepared by Clark and Wilkins.[32]

X-ray Crystal Structures of 1 and 3. An ORTEP plot of the $[SnMe_2Br_3]^-$ anion in complex **3** is shown in Figure 2, and selected bond lengths and angles are presented in Table 3. Although a highly anisotropic motion was noted for C(1), no evidence was found for split sites. In contrast to the structure of most $[SnMe_2Cl_3]^-$ anions, which are associated as dimers,[8c,16] the structure of **3** contains isolated $[SnMe_2Br_3]^-$ anions with the shortest intermolecular Sn···Br distance being 4.240(2) Å. In agreement with the spectroscopic results for **2**, the $[SnMe_2Br_3]^-$ anions have a trigonal-bipyramidal structure with the Me groups in equatorial positions. The structure has no axial symmetry, thus explaining the high asymmetry in the MAS ^{119}Sn NMR spectrum of **2**. The axial Sn−Br distances (2.734(2) Å) are significantly longer than the equatorial one (2.498(3) Å) as expected from the VSEPR model, which also accounts for the equatorial position of the (less electronegative) Me groups.[38] The C−Sn−C angle (133.2(8)°) is larger than the ideal angle of 120°, in agreement with the isovalent rehybridization principle,[39] which predicts that the tin atom will concentrate greater s character into the orbitals directed toward the less electronegative carbon atoms. The equatorial C−Sn−Br angles are smaller than 120°, to keep the sum of equatorial angles equal to 360°, and all the other bond angles are close to those corresponding to a regular trigonal bipyramid. The crystallographic study of **3** provides the first X-ray crystal structure containing an $[SnR_2Br_3]^-$ anion.

Figure 3 shows an ORTEP plot of the $[SnMe_2Br_4]^{2-}$ anion in complex **1**, and selected bond lengths and angles are collected in Table 4. The octahedral centrosymmetric anion has a crystallographically imposed linear C−Sn−C arrangement, in agreement with the mutual exclusion of ν_{as}(Sn−C) and ν_s(Sn−C) in the IR and Raman spectra but far from the C−Sn−C angle of 158° calculated from the Mössbauer QS (see above). However, the QS gives a good prediction of the average Sn−Br distance according to the published correlation,[2] as the calculated value of 2.78 ± 0.02 Å is close to the experimental average distance (2.7681(11) Å). The two Sn−Br distances are essentially identical, according to the estimated standard deviations, and the largest deviation of the bond angles from the ideal ones is 0.5(3)°. Therefore, the symmetry of the centrosymmetric $[SnMe_2Br_4]^{2-}$ anion is close to the idealized D_{4h}, in agreement with the axial symmetry found in the MAS ^{119}Sn NMR spectrum. A comparison of the structures of the $[SnMe_2Br_4]^{2-}$ and $[SnMe_2Br_3]^-$ anions in **1** and

(38) Gillespie, R. J.; Robinson, E. A. *Angew. Chem., Int. Ed. Engl.* **1996**, *35*, 495.
(39) Bent, H. A. *Chem. Rev.* **1961**, *61*, 275.

Table 5. SCF Energies (au) and Bond Distances (Å) and Angles (deg) for the Optimized Structures

compd	energy[a]	C−Sn−C	X−Sn−X	Sn−X	Sn−C
$SnMe_2F_2$	−131.393 00	124.9	102.3	1.929	2.123
$SnMe_2Cl_2$	−113.006 54	120.2	105.6	2.364	2.132
$SnMe_2Br_2$	−109.846 23	119.7	105.9	2.502	2.134
$SnMe_2I_2$	−305.887 53	117.7	108.2	2.733	2.138
$SnEt_2Cl_2$	−126.365 46	121.6	105.1	2.371	2.141
$[SnMe_2F_3]^-$	−155.459 31	128.7	87.9	2.043 (ax) 1.951 (eq)	2.142
$[SnMe_2Cl_3]^-$	−127.882 91	133.0	91.2	2.636 (ax) 2.398 (eq)	2.137
$[SnMe_2Br_3]^-$	−123.145 56	132.5	91.3	2.782 (ax) 2.537 (eq)	2.140
$[SnMe_2I_3]^-$	−417.211 80	133.5	93.3	3.097 (ax) 2.768 (eq)	2.143
$[SnEt_2Cl_3]^-$	−141.241 70	133.1	91.3	2.645 (ax) 2.398 (eq)	2.147
trans-$[SnMe_2F_4]^{2-}$	−179.363 05	180	90	2.092	2.165
trans-$[SnMe_2Cl_4]^{2-}$	−142.636 15	180	90	2.730	2.129
trans-$[SnMe_2Br_4]^{2-}$	−136.327 09	180	90	2.866	2.133
trans-$[SnMe_2I_4]^{2-}$	−528.433 51	180	90	3.180	2.133
trans-$[SnEt_2Cl_4]^{2-}$	−155.991 96	180	90.5	2.736	2.155
cis-$[SnMe_2Cl_4]^{2-}$	−142.605 41	100.6	83.2[b] 178.5[c] 90.6[d]	2.610[e] 2.691[f]	2.183
cis-$[SnEt_2Cl_4]^{2-}$	−155.962 47	93.3	82.4[b] 178.6[c] 90.5[d]	2.597[e] 2.696[f]	2.199

[a] Valence energy, which excludes the internal energy of the core electrons. The values are not corrected for zero-point energies. [b] Between Cl atoms trans to the R groups. [c] Between Cl atoms cis to the R groups. [d] Between one Cl atom cis and another trans to the R groups. [e] Trans to the R groups. [f] Cis to the R groups.

3, respectively, shows Sn−Br distances in the order Sn−Br_{eq} (2.498(3) Å) ≪ Sn−Br_{ax} (2.734(2) Å) < Sn−Br_{oct} (2.7681(11) Å). The differences in bond strength explain that only ν(Sn−Br_{ax}) appears above 200 cm^{-1} (218−221 cm^{-1}) in the IR and Raman spectra of the $[SnMe_2Br_4]^{2-}$ and $[SnMe_2Br_3]^-$ anions.

Solution Structures. The ^{119}Sn NMR spectrum of **2**, in $CDCl_3$ solution, displays a narrow resonance at −118.8 ppm. This value is close to the isotropic chemical shift in the MAS ^{119}Sn NMR spectrum (−135 ppm) and indicates pentacoordinated tin atoms.[36,37] The $^1J(^{119}Sn-^{13}C)$ and $^2J(^{119}Sn-^1H)$ coupling constants, from the ^{13}C and ^{1}H NMR spectra, lead to calculated C−Sn−C angles[40,41] of 132.3 and 134.9°, respectively. These values are very close to that found in the X-ray crystal structure of **3** (133.2°) and indicate very little structural change between the solid state and $CDCl_3$ solution. On the other hand, **3** was not soluble in $CDCl_3$.

In the case of complex **1**, a chemical shift of −144.1 ppm was found in the ^{119}Sn NMR spectrum of a $CDCl_3$ solution. This value is in the range of pentacoordinated diorganotin(IV) compounds[36,37] and close to the isotropic chemical shift in the MAS ^{119}Sn NMR spectrum of **2**. Furthermore, the calculated C−Sn−C angles, from the $^1J(^{119}Sn-^{13}C)$ and $^2J(^{119}Sn-^1H)$ coupling constants,[40,41] are 134.2 and 137.7°, respectively. These values are similar to those calculated for complex **2** and to the solid-state angle in **3**. Therefore, the $[SnMe_2Br_4]^{2-}$ anions in **1** are essentially dissociated in $CDCl_3$ solution into $[SnMe_2Br_3]^-$ and Br^- ions, although the different chemical shift values in the ^{119}Sn NMR spectra of **1** and **2** are suggestive of solution equilibria.

The ^{1}H NMR spectra of complexes **1**−**3**, in D_2O solution, display $^2J(^{119}Sn-^1H)$ coupling constants in the range 107.5−107.8 Hz, which indicate essentially linear C−Sn−C arrangements.[41] Furthermore, the ^{119}Sn chemical shifts of **1** and **2** (−324.9 and −322.3 ppm, respectively) are consistent with hexacoordinated tin atoms.[36,37] To understand this behavior, it is interesting to note that aqueous solutions of dialkyltin dihalides behave like 1:2 electrolytes with almost complete aquation, and the interaction of the $SnMe_2^{2+}$(aq) ion with Br^- is very weak, with $\log \beta_1 \approx -1.0$.[42] In addition, the hydrolysis of $[SnMe_2(H_2O)_4]^{2+}$ has been investigated by several authors, and the stability constants of the hydroxo species formed have been reported.[43] When one takes into account all the stability constants, the most abundant species in aqueous solutions of **1** and **2** must be octahedral $[SnMe_2(H_2O)_4]^{2+}$, although equilibrium mixtures are present. It is curious that by mixing $SnMe_2Br_2$ with Et_4NBr, in a 1:2 molar ratio, octahedral **1** crystallizes from $CHCl_3$ solutions, where pentacoordinated $[SnMe_2Br_3]^-$ anions are present, but pentacoordinated **2** crystallizes from aqueous solutions, where octahedral species are present.

Optimized Structures. The main energetic and structural results of the ab initio MO calculations are collected in Table 5. Most calculated bond distances are longer than the experimental ones, as often found for metal halides[44] and organotin compounds.[4,17] The differences are small for Sn−C distances and larger for the Sn−X distances. In addition to the lack of correction

(40) Lockhart, T. P.; Manders, W. F. *J. Am. Chem. Soc.* **1987**, *109*, 7015.
(41) Lockhart, T. P.; Manders, W. F. *Inorg. Chem.* **1986**, *25*, 892.
(42) Farrer, H. N.; McGrady, M. M.; Tobias, R. S. *J. Am. Chem. Soc.* **1965**, *87*, 5019.
(43) (a) Tobias, R. S.; Ogrins, I.; Nevett, B. A.; *Inorg. Chem.* **1962**, *1*, 638. (b) Yasuda, M.; Tobias, R. S. *Inorg. Chem.* **1963**, *2*, 207. (c) Tobias, R. S.; Yasuda, M. *Can. J. Chem.* **1964**, *42*, 781. (d) Arena, G.; Purrello, R.; Rizzarelli, E.; Gianguzza, A.; Pellerito, L. *J. Chem. Soc., Dalton Trans.* **1989**, 773. (e) Natsume, T.; Aizawa, S.-I.; Hatano, K.; Funahashi, S. *J. Chem. Soc., Dalton Trans.* **1994**, 2749. (f) Buzás, N.; Gajda, T.; Nagy, L.; Kuzmann, E.; Vértes, A.; Burger, K. *Inorg. Chim. Acta* **1998**, *274*, 167.
(44) Hargittai, M. *Chem. Rev.* **2000**, *100*, 2233.

for electron correlation effects, other factors account for the difference between calculated and experimental bond lengths. In particular, while chemical quantum calculations lead to the equilibrium internuclear distances, X-ray structure determinations lead to the thermally averaged distances, which are shorter than equilibrium distances because of librational motion.[45] For example, Dunitz has shown that the discrepancy between the calculated and X-ray C=C distances for the "shortest C=C double bond known in any hydrocarbon"[46] was largely due to neglect of corrections for molecular motion in the crystal.[47] Also, the Sn−Cl distances in a series of hexachlorostannate(IV) salts, obtained by the independent motion model, were longer than those obtained by conventional refinement, by 0.02−0.09 Å.[48] Furthermore, while the calculated equilibrium distances correspond to the gas-phase structure, solid-state structures are strongly affected by the environment and, in the case of ionic compounds, particularly by the counterion. Consequently, the calculated Sn−Cl distance for $SnMe_2Cl_2$ is close to that found in the gas-phase electron diffraction experiments (within 0.04 Å),[49] but the differences for the solid-state X-ray crystal structures of $[SnMe_2Cl_3]^-$ and $[SnMe_2Cl_4]^{2-}$ are in the ranges 0.08−0.10 Å[15] and 0.10−0.13 Å,[8] respectively. In the solid state, the effects of the crystal environment lead to standard deviations in the metal−ligand bond length on the order of 0.01−0.02 Å, while the corresponding values for the valence angles at the metal atoms typically lie in the range 1−2°.[18] In their comparison between solid-state and theoretical structures of organotin compounds, Tiekink and co-workers found that while bond angles subtended at tin did not change significantly, tin−ligand separations tended to elongate in the gas phase.[4,17] To interpret properly the bond distances in Table 5, we have to consider the "offset" method, which assumes that errors due to basis-set deficiency and electron correlation are atom-pair properties that are similar for different compounds containing the same bonds.[50] Therefore, the differences between bond lengths in different compounds are more reliable than the absolute computed values.

In the absence of solid-state effects, some structural features in Table 5 can be compared. For example, the structures of $SnMe_2X_2$ are consistent with the isovalent rehybridization principle,[39] which predicts that the tin atom will concentrate greater p character into the hybrid orbitals directed to the more electronegative halogens and greater s character into the orbitals directed to the carbon atoms. In this way, the C−Sn−C angles are larger than the ideal tetrahedral angle and become wider as the electronegativity of the halogen increases, while the X−Sn−X angles decrease and the Sn−C bonds become shorter. Therefore, C−Sn−C angles around 120° are normal for an isolated $SnMe_2X_2$ molecule. The present calculations are relevant to the question of whether the intermolecular Cl···Sn interactions in solid $SnMe_2Cl_2$ have significant structural consequences. On the basis of ^{13}C NMR data, the C−Sn−C angle was calculated to be 116.5° in solution in noncoordinating solvents and 122° in the solid state,[51] while the X-ray structure shows an angle of 123.5(45)°.[52] It was concluded that the magnitude of the change in structure on crystallization is small enough to be accounted for without invoking a significant bridging halide interaction.[51] Our gas-phase calculated C−Sn−C angle of 120.2° is close enough to the solid-state angle to strongly support the above conclusion (in the gas-phase structure determination, angles closer to the regular tetrahedral angle were reported, but they could not be determined with satisfactory accuracy).[49]

The optimized structures of $[SnR_2X_3]^-$ anions show a trigonal-bipyramidal geometry, with the R groups in equatorial positions and longer Sn−X distances for the axial bonds than for the equatorial ones. The difference between the axial and equatorial bond lengths is ca. 5% for $[SnMe_2F_3]^-$ and ca. 10% for the other anions. As one goes from SnR_2X_2 to the $[SnR_2X_3]^-$ anions, the C−Sn−C angle is further expanded while the $Sn-X_{eq}$ bond becomes only ca. 1.3% longer. For octahedral *trans*-$[SnR_2X_4]^{2-}$ anions, the Sn−X bonds are even longer (by ca. 3%) than the axial Sn−X bonds in the trigonal-bipyramidal $[SnR_2X_3]^-$ anions. Finally, for *cis*-$[SnR_2X_4]^{2-}$ (R = Me, Et), the Sn−Cl bonds cis to the R groups are longer than the trans bonds, in agreement with the cis weakening effect of the R groups previously found experimentally.[53] The average Sn−Cl distance in *cis*-$[SnR_2X_4]^{2-}$ is shorter, and the Sn−C distance longer, than for *trans*-$[SnR_2X_4]^{2-}$, in agreement with the idea that in *trans*-SnX_4L_2 complexes the Sn−L bonds are stronger and the Sn−X bonds are weaker than in their corresponding cis isomers.[54]

If we compare the X-ray crystal structures of **1** and **3** with the calculated gas-phase structures of the $[SnMe_2Br_4]^{2-}$ and $[SnMe_2Br_3]^-$ anions, we find, as expected, that the calculated distances are longer (by 0.039−0.098 Å for Sn−Br and less than 0.01 Å for Sn−C). Nevertheless, in both cases the Sn−Br distances are in the order $Sn-Br_{eq} \ll Sn-Br_{ax} < Sn-Br_{oct}$, with increases of 9.7 and 3.0% for calculated distances and 9.4 and 2.3% for the experimental ones. Therefore, if we subtract a fixed value of 0.07 Å from the computed Sn−Br distances, averaging all factors that lead to deviations between calculated and experimental distances (limitations in the calculation, librational motion, and packing effects), experimental and calculated distances agree within 0.03 Å. Furthermore, the calculated C−Sn−C angle for the $[SnMe_2Br_3]^-$ anion (132.5°) is in excellent agreement with both the X-ray solid-state angle (133.2(8)°) and the $CDCl_3$ solution angle calculated from ^{13}C NMR data (132.3°). In conclusion, the structure of the $[SnMe_2Br_3]^-$ anion is essentially the same in the solid state, in solution in noncoordinating

(45) Trueblood, K. N. In *Accurate Molecular Structures*; Domenicano, A., Hargittai, I., Eds.; Oxford University Press: Oxford, U.K., 1992; Chapter 8.
(46) Baldridge, K. M.; Biggs, B.; Bläser, D.; Boese, R.; Gilbertson, R. D.; Haley, M. M.; Maulitz, A. H.; Siegel, J. S. *Chem. Commun.* **1998**, 1137.
(47) Dunitz, J. D. *Chem. Commun.* **1999**, 2547.
(48) Brill, T. B.; Gearhart, R. C.; Welsh, W. A. *J. Magn. Reson.* **1974**, *13*, 27.
(49) Fujii, H.; Kimura, M. *Bull. Chem. Soc. Jpn.* **1971**, *44*, 2643.
(50) Jeffrey, G. A. In *Accurate Molecular Structures*; Domenicano, A., Hargittai, I., Eds.; Oxford University Press: Oxford, U.K., 1992; Chapter 11.
(51) Lockhart, T. P.; Farlee, R. D. *Inorg. Chem.* **1987**, *26*, 3226.
(52) Davies, A. G.; Milledge, H. J.; Puxley, D. C.; Smith, P. J. *J. Chem. Soc. A* **1970**, 2862.
(53) Buslaev, Yu. A.; Kravchenko, E. A.; Burtzev, M. Yu.; Aslanov, L. A. *Coord. Chem. Rev.* **1989**, *93*, 185.
(54) Tudela, D.; Tornero, J. D. *Inorg. Chim. Acta* **1993**, *214*, 197.

Table 6. Calculated Energy Changes (kJ/mol) for the Successive Formation of the $[SnR_2X_3]^-$ (ΔE_1) and $[SnR_2X_4]^{2-}$ (ΔE_2) Anions in the Gas Phase

X	R	ΔE_1	ΔE_2
F	Me	−270.1	+156.5 (trans)
Cl	Me	−127.0	+196.1 (trans)
			+276.7 (cis)
Br	Me	−114.5	+194.6 (trans)
I	Me	−72.4	+196.4 (trans)
Cl	Et	−126.7	+203.9 (trans)
			+281.3 (cis)

solvents, and in the gas phase. When one takes into account that calculated distances are longer than the experimental ones, the present results strongly support the accuracy of the structural predictions from ab initio MO calculations.

Although calculated Sn−X distances are longer than experimental ones, the calculated Sn−F distance in $[SnMe_2F_4]^{2-}$ (2.092 Å) is shorter than those found in the X-ray crystal structure of $(NH_4)_2[SnMe_2F_4]$ (2.121(5)−2.135(4) Å).[12a] This fact highlights the significant lengthening of the Sn−F distances under the influence of the N−H···F hydrogen bonds.[12a]

Computed Gas-Phase Energetics. The successive formation of the $[SnR_2X_3]^-$ and $[SnR_2X_4]^{2-}$ anions in the gas phase is represented by eqs 1 and 2, and the

$$SnR_2X_2 + X^- \rightarrow [SnR_2X_3]^- \qquad \Delta E_1 \qquad (1)$$

$$[SnR_2X_3]^- + X^- \rightarrow [SnR_2X_4]^{2-} \qquad \Delta E_2 \qquad (2)$$

calculated energy changes are shown in Table 6. While the formation of the pentacoordinated $[SnR_2X_3]^-$ anions is an exothermic process, the formation of octahedral $[SnR_2X_4]^{2-}$ is endothermic. Therefore, $[SnR_2X_4]^{2-}$ ions are unstable in the gas phase toward dissociation into $[SnR_2X_3]^-$ and X^-, and their existence in the solid state must be due to the higher lattice energy of $M_2[SnR_2X_4]$ salts as compared to $M[SnR_2X_3]$. Indeed, it has been concluded that many multiply charged anions, including many commonly proposed in condensed media, do not exist as stable moieties in the gas phase.[55] It may be surprising that such common species as octahedral $[SnR_2X_4]^{2-}$ anions are unstable in the gas phase, but we have also found that $[SnMe_2Br_4]^{2-}$ anions are unstable toward dissociation into $[SnMe_2Br_3]^-$ and Br^- in $CDCl_3$ solution (see above). It can be seen in Tables 5 and 6 that *cis*-$[SnR_2Cl_4]^{2-}$ species (R = Me, Et) are unstable with respect to their trans isomers by ca. 79 kJ/mol, thus explaining the ubiquitous *trans*-R−Sn−R arrangement. The more electronegative the halogen is, the more exothermic the formation of $[SnR_2X_3]^-$ anions. Indeed, a very good linear correlation ($r = 0.997$) is obtained between ΔE_1 and the Allred−Rochow electronegativity of X,[56] with a maximum deviation of 7.7 kJ/mol for X = I, while the range of calculated ΔE_1 values spans 197.7 kJ/mol. There is no reason for the correlation to be linear, and indeed, a polynomial correlation fits even better ($r^2 = 0.9996$), with a maximum deviation of 2.0 kJ/mol for X = Cl. This behavior agrees with the idea that the more electronegative the halogen X is, the stronger the Lewis acidity of the SnR_2Cl_2 molecule. This tendency should also be present in reaction 2, but the Coulomb repulsion between $[SnR_2X_3]^-$ and X^- becomes greater as the halogen X becomes smaller, and a compromise between both factors leads to the unexpected result that ΔE_2 is essentially constant for X = Cl, Br, I (see Table 6).

Thermochemical Calculations. The results in Table 6 allow a more quantitative analysis of the cycle shown in Figure 1, because ΔH_{dis} can be estimated. Bearing in mind that the correction for zero-point energy for ΔE_2 is small and counterbalancing the transformation of energy change into enthalpy change, we can approximate $\Delta H_{dis} \approx -\Delta E_2$. On the other hand, the lattice potential energies, $U_{pot} + 3RT$ for $(Et_4N)_2[SnMe_2Br_4]$ and $U_{pot} + 2RT$ for $(Et_4N)[SnMe_2Br_3]$,[57] can be estimated from the molecular volumes using the recently published correlations.[57] In the case of **1**, the unit cell volume and *Z* value in Table 1 lead to a molecular volume of 0.717 15 nm^3 and a calculated U_{pot} of 929 kJ/mol.[57] Although the crystal structure of **2** could not be solved, the unit cell volume and *Z* value in Table 1 lead to a molecular volume of 0.446 65 nm^3 and a calculated U_{pot} of 411 kJ/mol.[57] As suggested above, the higher lattice energies of $M_2[SnR_2X_4]$ salts as compared to those of $M[SnR_2X_3]$ are responsible for the existence of $M_2[SnR_2X_4]$ in the solid state. In the case of aqueous solutions, the sum of the hydration enthalpies of the Et_4N^+ and Br^- ions can be calculated to be −542 kJ/mol from the enthalpy of solution in water of Et_4NBr (6.05 kJ/mol) and the enthalpies of formation of gaseous Br^- (−219.09 kJ/mol) and Et_4N^+ (424 kJ/mol) and crystalline Et_4NBr (−342.7 kJ/mol).[58] With the values $\Delta H_{lat}(1:2) = 936$ kJ/mol, $\Delta H_{lat}(1:1) = 416$ kJ/mol, $\Delta H_{dis} = -195$ kJ/mol, and $\Delta H_{hydr}(Br^-) + \Delta H_{hydr}(Et_4N^+) = -542$ kJ/mol, ΔH in Figure 1 is calculated to be −217 kJ/mol for aqueous solutions at 298 K. Furthermore, the entropy terms favor the dissociation of $(Et_4N)_2[SnMe_2Br_4]$, thus explaining that the reaction of $SnMe_2Br_2$ with Et_4NBr, in a 1:2 molar ratio, yields $(Et_4N)[SnMe_2Br_3]$ in water. Nevertheless, $\Delta H_{lat}(1:2) + \Delta H_{dis} - \Delta H_{lat}(1:1) = +325$ kJ/mol, and ΔH in Figure 1 can be positive in solvents with low solvating power. For that reason, when the reaction is performed in $CHCl_3$/hexane mixtures, crystalline $(Et_4N)_2[SnMe_2Br_4]$ is formed.

Similar calculations can be performed for the Me_4N^+ salts, although the unit cell constants of $(Me_4N)_2[SnMe_2Br_4]$ are not known. From the molecular volumes of 10 Et_4N^+ salts[59] and the tabulated anion volumes,[57] the ion volume for Et_4N^+ is 0.215 ± 0.006 nm^3. With this value and the molecular volume of **1** (0.717 15 nm^3), we obtain a value of 0.287 nm^3 for the ion volume of

(55) Boldyrev, A. I.; Gutowski, M.; Simons, J. *Acc. Chem. Res.* **1996**, *29*, 497.

(56) Huheey, J. E.; Keiter, E. A.; Keiter, R. L. *Inorganic Chemistry*, 4th ed.; Harper Collins: New York, 1993; p 187.

(57) Jenkins, H. D. B.; Roobottom, H. K.; Passmore, J.; Glasser, L. *Inorg. Chem.* **1999**, *38*, 3609.

(58) Nagano, Y.; Sakiyama, M.; Fujiwara, T.; Kondo, Y. *J. Phys. Chem.* **1988**, *92*, 5823.

(59) (a) Giuseppetti, G.; Tadini, C.; Ferloni, P.; Zabinska, G.; Torre, S. *Z. Kristallogr.* **1994**, *209*, 509. (b) Sowa, H.; Druck, U.; Kutoglu, A. *Z. Kristallogr.* **1981**, *154*, 333. (c) Vincent, B. R.; Knop, O.; Linden, A.; Cameron, T. S.; Robertson, K. N. *Can. J. Chem.* **1988**, *66*, 3060. (d) Eichler, W.; Seifert, H. J. *Z. Anorg. Allg. Chem.* **1977**, *431*, 123. (e) Elyoubi, M. S. D.; Ben Ghozlen, M. H.; Mlik, Y.; Daoud, A. *Phys. Status Solidi A* **1986**, *98*, 435. (f) Bettinelli, M.; Di Sipio, L.; Valle, G.; Aschieri, C.; Ingletto, G. *Z. Kristallogr.* **1989**, *188*, 155. (g) Ruhlandt-Senge, K.; Bacher, A.-D.; Muller, U. *Acta Crystallogr., Sect. C.* **1990**, *46*, 1925. (h) Cotton, F. A.; Diebold, M. P.; Roth, W. J. *Acta Crystallogr., Sect. C.* **1990**, *46*, 1624. (i) Srivastava, P. C.; Schmidt, H.-G.; Roesky, H. W. *Z. Naturforsch., B: Anorg. Chem., Org. Chem.* **1995**, *50*, 695.

$[SnMe_2Br_4]^{2-}$, which agrees with the 0.278 nm^3 obtained from the unit cell data of $Cs_2[SnMe_2Br_4]$,[60] thus giving an average value of 0.283 ± 0.005 nm^3 for the ion volume of $[SnMe_2Br_4]^{2-}$. From the molecular volumes of 17 Me_4N^+ salts[61] and the tabulated anion volumes,[57] the ion volume of Me_4N^+ is 0.126 ± 0.018 nm^3. Consequently, the calculated molecular volume and U_{pot} value[57] for $(Me_4N)_2[SnMe_2Br_4]$ are 0.535 nm^3 and 1043 kJ/mol, respectively. On the other hand, the unit cell volume and Z value for **3** in Table 1 lead to a calculated U_{pot} value of 435 kJ/mol for **3**.[57] Therefore, taking into account the RT terms, $\Delta H_{lat}(1:2) = 1050$ kJ/mol and $\Delta H_{lat}(1:1) = 440$ kJ/mol. The sum of the hydration enthalpies of the Me_4N^+ and Br^- ions can be calculated to be −554 kJ/mol from the enthalpy of solution in water of Me_4NBr (24.27 kJ/mol) and the enthalpies of formation of gaseous Br^- (−219.09 kJ/mol) and Me_4N^+ (546 kJ/mol) and crystalline Me_4NBr (−251.0 kJ/mol).[58] In the case of Me_4N^+ ions, ΔH in Figure 1 is calculated to be −139 kJ/mol for aqueous solutions at 298 K, thus explaining that the reaction of $SnMe_2Br_2$ with Me_4NBr, in a 1:2 molar ratio, yields $(Me_4N)[SnMe_2Br_3]$ in water. The crystallization of $(Me_4N)[SnMe_2Br_3]$ ($\Delta H = -139$ kJ/mol) is less favorable than that of $(Et_4N)[SnMe_2Br_3]$ ($\Delta H = -217$ kJ/mol), because the smaller volume of the Me_4N^+ ion leads to a higher lattice enthalpy for $(Me_4N)_2[SnMe_2Br_4]$. Of course, this compound would have crystallized from $CHCl_3$/hexane mixtures if Me_4NBr had been soluble in $CHCl_3$. From the molecular volumes of **2** and **3**, obtained from the cell volumes and Z values in Table 1, and the ion volumes of Et_4N^+ (0.215 nm^3) and Me_4N^+ (0.126 nm^3), we obtain a ion volume of 0.231 nm^3 for $[SnMe_2Br_3]^-$, smaller than that of $[SnMe_2Br_4]^{2-}$ (0.283 nm^3), as expected.

Acknowledgment. We are grateful to Drs. J. M. Calleja and J. D. Tornero (Universidad Autónoma de Madrid) and Dr. I. Sobrados (Instituto de Ciencias de Materiales de Madrid, CSIC) for recording the Raman, Mössbauer, and ^{119}Sn MAS NMR spectra, respectively, and Drs. H. D. B. Jenkins (University of Warwick, Warwick, U.K.) and A. Lyčka (Research Institute for Organic Syntheses, Pardubice, Czech Republic) for helpful comments. Computer time from the CCCFC (Universidad Autónoma de Madrid) and financial support from the Spanish Dirección General de Enseñanza Superior (Projects PB97-0067 and PB98-0108) and the Russian Fund of Basic Research (Grant 00-03-32578) are gratefully acknowledged.

Supporting Information Available: Tables giving details of crystal structure determinations, atomic coordinates, thermal parameters, bond lengths, and bond angles for **1** and **3**. This material is available free of charge via the Internet at http://pubs.acs.org.

OM000808S

(60) Hobbs, C. W.; Tobias, R. S. *Inorg. Chem.* **1970**, *9*, 1037.

(61) (a) Furukawa, Y.; Prabhumirashi, L. S.; Ikeda, R.; Nakamura, D. *Bull. Chem. Soc. Jpn.* **1982**, *55*, 995. (b) Abriel, W. *Z. Naturforsch., B* **1986**, *41*, 592. (c) Trouelan, P.; Lefebvre, J.; Derollez, P. *Acta Crystallogr., Sect. C* **1984**, *40*, 386. (d) Paseshnitchenko, K. A.; Aslanov, L. A.; Jatsenko, A. V.; Medvedev, S. V. *J. Organomet. Chem.* **1985**, *287*, 187. (e) German, K. E.; Grigor'ev, M. S.; Kuzina, A. F.; Gulev, B. F.; Spitsin, V. I. *Dokl. Akad. Nauk SSSR* **1986**, *287*, 650. (f) Malchus, M.; Jansen, M. *Z. Naturforsch., B* **1998**, *53*, 704. (g) Kornath, A.; Blecher, O. *Z. Naturforsch., B* **1999**, *54*, 372. (h) Wilson, W. W.; Christe, K. O.; Feng, J.; Bau, R. *Can. J. Chem.* **1989**, *67*, 1898. (i) Giuseppetti, G.; Mazzi, F.; Tadini, C.; Ferloni, P.; Torre, S. *Z. Kristallogr.* **1992**, *202*, 81. (j) Batchelor, R. J.; Einstein, F. W. B.; Gay, I. D.; Jones, C. H. W.; Sharma, R. D. *Inorg. Chem.* **1993**, *32*, 4378. (k) Nielsen, K.; Berg. R. W. *Acta Chem. Scand., Ser. A* **1980**, *34*, 153. (l) Malchus, M.; Jansen, M. *Acta Crystallogr., Sect. B* **1998**, *54*, 494. (m) Herrschaft, G.; Hartl, H. *Acta Crystallogr., Sect. C* **1989**, *45*, 1021. (n) Berg, R. W.; Nielsen, K. *Acta Chem. Scand., Ser. B* **1979**, *33*, 157. (o) Wiesner, J. R.; Srivastava, R. C.; Kennard, C. H. L.; di Vaira, M.; Lingafelter, E. C. *Acta Crystallogr.* **1967**, *23*, 565. (p) Madariaga, G.; Zuniga, F. J.; Perez-Mato, J. M.; Tello, M. J. *Acta Crystallogr., Sect. B* **1987**, *43*, 356. (q) Hasebe, K.; Mashiyama, H.; Koshiji, N.; Tanisaki, S. *J. Phys. Soc. Jpn.* **1987**, *56*, 3543. (r) Cheban, Yu. M.; Dvorkin, A. A.; Rotaru, V. K.; Malinovskii, T. I. *Kristallografiya* **1987**, *32*, 1027. (s) Evans, D. J.; Hughes, D. L. *Acta Crystallogr., Sect. C* **1990**, *46*, 1452. (t) Stammler, M. *J. Inorg. Nucl. Chem.* **1967**, *29*, 2203.